Interplay of computer simulations and x-ray absorption spectra in the study of the bromide hydration structure

Patrick J. Merkling, Regla Ayala, José M. Martínez, Rafael R. Pappalardo, and Enrique Sánchez Marcos[a)]
Departamento de Química Física, Universidad de Sevilla, 41012-Sevilla, Spain

(Received 4 April 2003; accepted 1 July 2003)

X-ray absorption spectra (EXAFS and XANES) were generated from snapshots of a Monte Carlo (MC) simulation of a bromide ion aqueous solution and from model structures. The MC simulation relies on a recently developed and tested polarizable potential based on *ab initio* potential energy surfaces. A comparison with the experimental *K*-edge Br spectrum of a 0.3 M YBr_3 aqueous solution was performed. XANES spectra are reproduced acceptably only if statistical fluctuations are included, which is performed in this work by using snapshots from computer simulation. As expected, single scattering BrO contributions are dominant in the case of the EXAFS region. Due to this fact, Br^- in water is a good model system for studying the influence of the distribution of distances on the determination of structural parameters. Then, a parallel study of the data analysis procedure of the experimental EXAFS spectrum and those theoretically computed from the structures supplied by the MC simulation, was carried out. The shape of the distribution function and its asymmetry must be taken into account in a practical way to obtain a more accurate determination of the BrO first-shell distance. A further refinement consists in using the computer simulation to extrapolate the BrO distance from the experimental EXAFS spectrum. In this way, a BrO distance of 3.44 ± 0.07 Å and a coordination number of 6 ± 0.5 were determined. © *2003 American Institute of Physics.* [DOI: 10.1063/1.1603719]

I. INTRODUCTION

The structure of ionic solutions has been a matter of increasing interest from experimental and theoretical points of view.[1–3] The main experimental techniques for structural studies of such systems are x-ray diffraction (XRD), neutron diffraction (ND), and x-ray absorption spectroscopy (XAS). Although XRD and ND can yield structural information about disordered systems like most liquids, their accuracy decreases strongly in the case of multicomponent systems (XRD) or requires considerable synthetic efforts to perform the isotopic substitutions (ND).[4,5] This fact restricts their use, as does the need for relatively high concentrations. Since the 1980s, one of the XAS techniques, extended x-ray absorption fine structure (EXAFS), has been applied to determine the pseudopartial pair correlation functions of atoms in both crystalline and amorphous systems.[6] Because XAS is element-specific, the local structure around one type of atom can be obtained by EXAFS. Additionally, it can be applied to a large range of concentrations, ranging typically from a few millimolar to several molar.

X-ray absorption spectroscopy has traditionally been subdivided, according to two energy regions of a spectrum: x-ray absorption near-edge structure (XANES), which corresponds to the near-edge region that extends from the threshold to about 50 eV above the edge, and EXAFS, which extends from energies of about 50 to more than 1000 eV above the edge. Since the kinetic energy of the photoelectron is low in the XANES region, multiple scattering (MS) effects are dominant, that in the particular case of ionic solutions are mostly due to scattering pathways between atoms of the first and second solvation shells around the absorber atom. In the XANES region, both geometrical and electronic details affect the shape of a spectrum, and therefore there is no general, direct, relationship between spectrum and geometry as in the case of EXAFS.[7] This is why the technique is often used as a fingerprint for characterizing the neighborhood of the absorber atom.[8]

In the EXAFS region, the scattered photoelectron has a high kinetic energy, so that single backscattering processes are dominant. However, multiple scattering phenomena may contribute noticeably to the spectrum, making its interpretation more difficult. In order to extract information contained in an EXAFS spectrum, a number of simplifying assumptions have to be made. Bearing in mind that the number and correlation of variables needed in the EXAFS analysis is often superior to the information contained in the EXAFS spectrum,[7,9–11] the use of information derived from other sources, like computational methods, is of special interest. This procedure has proven to be successful in many studies of structural elucidation of solid and liquid systems.[12–17]

The aim of this work is to obtain the bromide hydration structure by means of the combination of experimental information derived from XAS techniques and theoretical data from computer simulations. When dealing with the structural description of ionic solutions, the patterns for the cation and anion hydration are far from similar, mostly due to two reasons. First of all, anion environment is mainly determined by the resultant force of the competition between ion–dipole in-

a)Electronic mail: sanchez@simulux.us.es

teractions, which tend to favor symmetric hydrogen atoms arrangements around the anion-oxygen axis, and hydrogen bonding to the anion, which favors an asymmetric arrangement of its surrounding water molecules to maximize the hydrogen bond interaction. The second reason is that the electron density distribution is more expanded around the nucleus in the anion case what results in more important first- and second-order perturbations with respect to the local electric fields. These two reasons anticipate noticeable differences in the solvent organization around cations and anions, in particular of monoatomic or simple ions. In addition, the weak bromide–water interactions imply extremely fast solvent-exchange rates of the first solvation shell. All these reasons make the XAS study of the bromide hydration quite different from the study of highly charged cations previously carried out by our group.[18–25] Obviously, the sensitivity of the EXAFS technique to the disorder makes the structural analysis of this system more difficult. Thus, the use of theoretical information is expected to shed light on it.

Several authors have previously examined the bromide hydration with the help of theoretical tools. Wallen *et al.*[26] used molecular dynamics simulations to generate theoretical EXAFS spectra with the program FEFF and the evolution as a function of pressure and temperature of EXAFS and XANES spectra was analyzed. D'Angelo *et al.*[27] studied also EXAFS spectra with the program GNXAS, and combined MD simulation results with a short range model distribution based on Gamma functions to fit the EXAFS spectrum. However, none of them calculated the bromide XANES spectrum.

One of the most common assumptions made to calculate XAS spectra is to reduce the system to a single structure. Nevertheless, the contribution from molecules and arrangements instantaneously distorted has an important effect on the average spectrum,[22,25] especially in labile structures like the bromide ion hydration. In this sense, the possibility of considering statistical information makes the analysis procedure easier. A recently developed bromide–water interaction potential, which included the polarizability of particles based on *ab initio* data and whose good behavior has recently been checked by computer simulations,[28] will be employed in this combined experimental–theoretical study. It is worth pointing out that the theoretical spectra are computed from first principles, since no empirical parameters were introduced neither in the intermolecular potentials, nor in the computation of the XAS spectra. The XANES spectrum will be computed from a representative set of geometries extracted from the statistical trajectory. With respect to the EXAFS analysis, on one side the MD potential shall be probed, on the other side, details of the structural determination will be investigated.

II. METHODOLOGY

Theoretical XANES and EXAFS spectra of the Br *K*-edge (13 474 eV) are calculated by a combination of statistical and quantum-mechanical calculations. The study of the bromide hydration was performed using three approaches: (i) computation of XANES structures from quantum-mechanically minimized clusters with n water molecules ($4 \leqslant n \leqslant 7$); (ii) computation of XANES spectra taking into account the statistics through Monte Carlo simulation snapshots; (iii) analysis of EXAFS spectra in two ways: on the one hand, the experimental spectrum was compared to a theoretically computed one from Monte Carlo simulation snapshots; on the other hand, the fitting procedure of the EXAFS spectrum was carried out on both spectra, the experimental one and the one computed from Monte Carlo simulations. The comparison of the fits was carried out with the aim of testing the validity of the model structures used to describe the bromide hydration.

The experimental Br *K*-edge XAS spectra used in this work for 0.3 M aqueous solutions of YBr_3 were measured at beamline BL12C of the Photon Factory in Tsukuba, Japan. The ring current was 300 mA, and the ring energy 2.5 GeV. A high resolution Si (311) channel-cut monochromator was used. Calibration was carried out with the L_2-edge of a Au foil (13734 eV). Data were collected in transmission mode using ionization chambers as detectors.

The quantum-mechanically optimized structures used for obtaining XANES spectra were taken from a previous study on the microsolvation of the bromide ion in water, methanol, and acetonitrile.[29] In this study, $[Br(H_2O)_n]^-$ clusters ($1 \leqslant n \leqslant 8$) were optimized at the B3LYP level with double-ζ basis sets augmented with polarization and diffuse functions.

Statistical information was obtained from Monte Carlo (MC) simulations using first-principles bromide–water interaction potentials recently developed by our group.[28] For this potential, the Mobile Charge Density in Harmonic Oscillators Model was employed to describe bromide anion and water species, both of them being polarizable, and the water flexible. The water–water interactions were described by a MCDHO potential previously described by the Cuernavaca group, Mexico.[30] The reliability of the results derived from numerical simulations depends critically on the potential model describing the interactions among the sites defining the system. The interaction potential used has already been tested in previous studies,[28] where the simulated systems show a good agreement with experimental estimations. The MC simulations were carried out with the MCHANG program developed by the group of Cuernavaca.[31] The system simulated consists of $1\,Br^- + 211$ water molecules in the NVT ensemble at 300 K using the POT_2 interaction potential from Ref. 28. Periodic boundary conditions were applied, and long-range interactions were computed by the Ewald sum method, including a term to account for the net charge of the system.[32,33] Further details about the MC simulations are given in Ref. 28.

K-Edge XANES spectra of Br^- in water were calculated from 40 snapshots taken every 120 K ($K \equiv 10^3$) configurations of a MC simulation. The simulated XANES spectrum is an average over the spectra of the snapshots. XAS spectra have been computed with the FEFF8.10 program code[34] developed by Rehr's group. The potential calculations use the Hedin–Lundqvist self-energy approximation.[35] A self-consistent field procedure (SCF) was employed. A 6.0 Å cutoff radius was chosen for the SCF treatment and for the full-multiple scattering paths, ensuring the inclusion of the second solvation shell in the computation of the spectra. A muffin-tin potential was applied with overlap criteria of 1.0

(touching spheres), 1.15 and 1.15 for Br, O, and H atoms, respectively. These criteria were determined ad hoc but could be justified with the ionic nature of the absorbing atom. It was found that the SCF radius could be lowered to 5.0 Å without affecting the results. A XANES spectrum calculated from 200 snapshots taken every 250 K configurations and SCF cutoff of 5.0 Å yields very similar results.

In previous studies on cation hydration structure,[12,22,24,25] the inclusion of hydrogen atoms proved necessary for obtaining a realistic backscattering potential but led to a sensible degradation of the spectrum when they were included as backscatterers. Difficulties are mainly associated with an overestimation of the backscattering contribution, but this does not affect their role in the self-consistent field calculation of the potential.[16] In the case of bromide hydration structure, our results using the FEFF program indicated that the simulated spectra are more similar to the experimental ones (both EXAFS and XANES) when hydrogen atoms are included as backscatterers. Other authors, who do not use the same methodological approach to compute the EXAFS spectra, work with the assumption of using hydrogen atoms as backscatterers in both anion and cation studies.[17] The different strategy handling cation and anion hydration, apart from its heuristical justification as seen in Figs. 3 and 4, could be understood by the presence of a closest hydrogen shell around the anion. The bromide ion induces the presence of a set of hydrogen atoms of first-shell water molecules in its closest vicinity, which are found to play a significant role in both the photoelectron scattering phenomenon and the determination of electronic wave functions of the bromide clusters.

A simplified expression of the EXAFS function is given by[6]

$$\chi(k)=\sum_j \frac{N_j}{kR_j^2} S_0^2(k) F_j(k) e^{-2\sigma_j^2 k^2} e^{-2R_j/\lambda(k)} \sin(2kR_j + \varphi_j(k)), \quad (1)$$

where $\chi(k)$ is the total amplitude as a function of the vector k and the summation goes over all paths j. N_j is the coordination number, R_j is half of the path length, $S_0^2(k)$ is the amplitude reduction factor, $F_j(k)$ is the backscattering amplitude, σ_j^2 is the second-order cumulant known as the Debye–Waller (DW) factor, $\lambda(k)$ the mean free path of the photoelectron, and $\varphi_j(k)$ the phase-shift.

In Eq. (1), the disorder is described by the DW factor. Nonetheless, when theoretical information derived from numerical simulations is considered, structural fluctuations around the anion are implicit within the sampling of the configurational space. Then, the EXAFS function can be alternatively expressed as[22]

$$\chi(k)=\frac{1}{N_s}\sum_i^{\text{struc}} \sum_{j'}^{\text{paths}} \frac{N_{j'}}{kR_{ij'}^2} S_0^2(k) F_{j'}(k) e^{-2R_{ij'}/\lambda(k)} \times \sin(2kR_{ij'} + \varphi_{j'}(k)), \quad (2)$$

where N_s is the number of structures considered [in this case $\sim 10\,000$ structures evenly spaced over 50 M ($\mathrm{M} \equiv 10^6$) MC configurations], i goes over the structures derived from the statistical sampling, and j' over the paths. The role played by the exponential containing the DW factor of Eq. (1) is replaced by an average over structures in Eq. (2). In order to check the convergence of the results, a computation with 40000 structures evenly spaced over 200 M configurations was also performed. No differences were found between both averaged spectra. Further examples of this averaging over simulated spectra may be found in Refs. 12, 15, 26, 36, and 37.

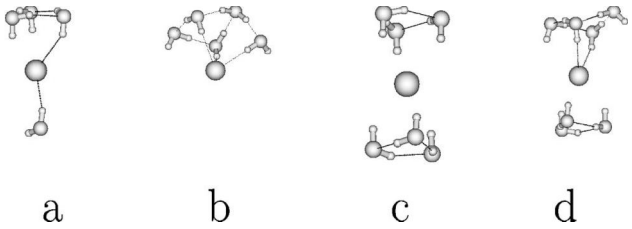

FIG. 1. Geometries of the quantum-mechanically optimized structures used to calculate XANES spectra of Fig. 2(a).

The cut-off radii selected were the same as those chosen in the XANES spectra. The considered paths were restricted to a length of up to 7.0 Å and an amplitude of at least 9% of the intensity of the shortest BrH path.

Structural parameters were obtained from both experimental and theoretical spectra by means of fitting a model structure to Eq. (1). Contact ion pairs could be excluded, as appeared as well from the analysis of the Y K-edge.[38] Thus, the model structure chosen is the hexahydrated cluster **c** depicted in Fig. 1. EXAFS data were analyzed with the FEFFIT 2.55 software package.[39] The fitting of the experimental EXAFS signal to Eq. (1) is based on a standard nonlinear least squares technique well-established in the literature.[40]

III. RESULTS AND DISCUSSION

A. XANES spectra

Calculated XANES spectra from a series of quantum-mechanically minimized structures containing between 4 and 7 water molecules are displayed in Fig. 2(a) and compared with the experimental spectrum. The geometries of the structures selected are shown in Fig. 1. The calculated XANES spectra show noticeable differences, especially with respect to the relative intensity of the resonances. To the contrary, the energy values of the first two resonances which appear at 13 472 and 13 489 eV, respectively, are reproduced reasonably well by all of them and are in agreement with the experimental spectrum. The comparison with the experimental spectrum shows that the ratio of the heights of the resonances is not reproduced. What is more, the main resonance of the experimental spectrum is wider and higher than the ones of the computed spectra.

XANES spectra are generally considered to be insensitive to disorder, but characteristic of the coordination geometry. In the case of bromide hydration, where the hydration structure is not well defined, the sensitiveness of the XANES spectrum to the instantaneous geometries can be illustrated on three structures picked out of the 40 considered to calcu-

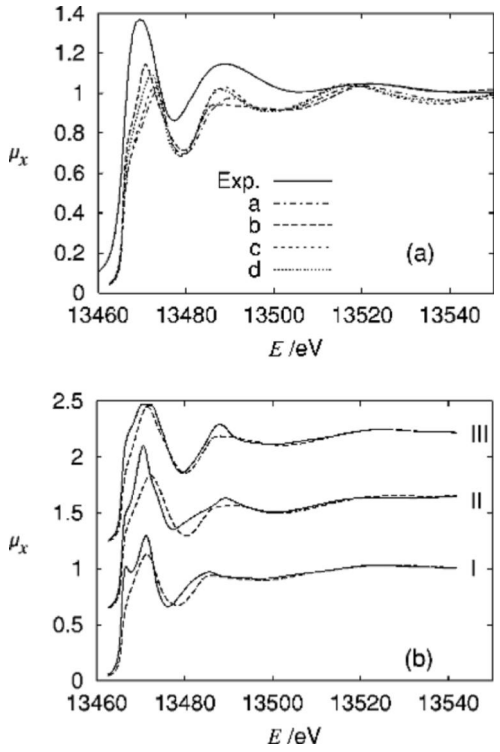

FIG. 2. Experimental Br K-edge XANES (solid line) and the ones computed from quantum-mechanically optimized structures shown in Fig. 1. (b) Individual XANES spectra computed for different snapshots, either restricted to first hydration shell (dashed lines) or not (solid lines).

late the average statistical spectrum [Fig. 2(b)]. On the one hand, and unlike the case of the quantum-mechanically optimized clusters, some of the individual spectra exhibit more intense resonances than the experimental one. On the other hand, the individual XANES spectra differ more between each other, than those computed from quantum-mechanical structures. This sensitivity of the XANES spectra to geometrical changes (from the fluctuations of the system) supports strongly the need to include statistical information in the simulation of XANES spectra of bromide solutions. If a unique model structure had been taken into consideration, the discrepancies between theoretical and experimental spectra would have been ascribed to the approximations considered in the quantum computations needed to generate the spectrum, and eventually, the semiempirical approximations introduced in obtaining some of the parameters. In the same figure, the computed spectra using the structures truncated to the first solvation shell are shown. The individual spectra are strongly affected by the truncation, what illustrates how XANES is sensitive to the solvation beyond the first shell, as already observed in the case of cation hydration.[24,25]

In Fig. 3, the comparison of the averaged calculated spectrum from statistical information and the experimental one is shown. Both the position of the two main resonances and the ratio of their heights agree. As expected from the qualitative analysis of the methodology used, the width of the main resonance of the averaged statistical spectrum is more similar to the experimental one than that obtained from a unique structure. Nevertheless, the fact that the intensity of

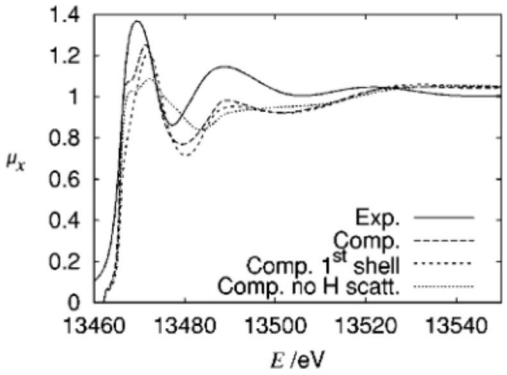

FIG. 3. Experimental Br K-Edge XANES (solid line) and computed from MC simulations, either using first hydration shell (short dashed line), or up to 6 Å (long dashed line). The hypothetical case where H atoms are not included as backscatterers is shown in dotted lines.

the main resonance increases when a great number of spectra derived from different structures is included, is striking.

In order to study the sensitivity of the XANES region to the absorber-backscatterer distance, the XANES spectrum has been recalculated considering the same points of the configurational space, but including only solvent molecules of the first solvation shell. According to the radial distribution function of the MC simulations,[28] a molecule belongs to the first solvation shell when the BrO distance is lower than 4.1 Å. The averaged spectrum obtained is included in Fig. 3 (short dashed line) and differs slightly from the one containing more than one hydration shell (dashed line). This behavior is different from the one found by our group in the study of cation hydration.[22,24,25] In the latter case, spectra calculated from structures that contained only one solvation shell presented a more intense maximum, and a slight displacement and narrowing of the main resonance was observed. The effect of the water molecules beyond the first hydration shell on the averaged XANES spectrum is small in the case of the bromide hydration, unlike what is observed when computing the effect of higher shells for individual snapshots. Thus, it does not seem possible to retrieve nontrivial structural information beyond the first hydration shell for this anion in studies of solution chemistry. The calculated XANES spectrum using a cutoff radius of 6.0 Å, where hydrogen atoms were not included as backscatterers, is also plotted in Fig. 3 (dotted lines). This computed spectrum differs significantly from the other spectra included in the figure.

B. EXAFS spectra

The comparison of the experimental and theoretical EXAFS spectra in terms of $\chi(k)\cdot k^2$ is displayed in Fig. 4. The agreement between both spectra is satisfactory, especially considering that no empirical parameters were included in the computation of the theoretical spectrum. When H atoms are excluded as backscatterers, the agreement is found to be far from satisfactory, supporting the importance of hydrogen atoms in the XAS spectra of the halide aqueous solutions.[41–44] As highlighted in these previous works, this is

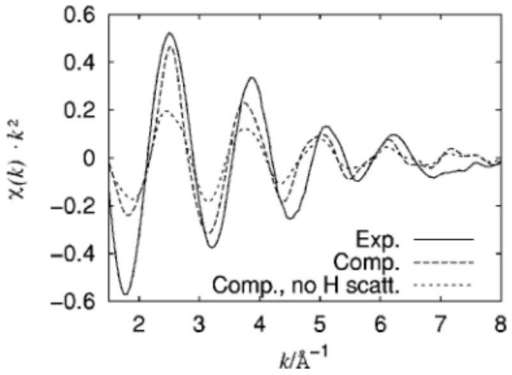

FIG. 4. Comparison of the experimental (solid line) and computed (long dashed line) k^2-weighted EXAFS function. When H atoms are not included as backscatterers, the EXAFS function would be represented by the short dashed line.

due to the nearly linear alignment of atoms BrHO and as a consequence, the hydrogen atom has a focusing effect for the photoelectron wave.

Figure 5(a) displays the experimental spectrum and its fit using as a model structure cluster "c" of Fig. 1. In Fig. 5(b), the phase-corrected Fourier transform (FT) along with its fit are plotted. A summary of the structural parameters obtained

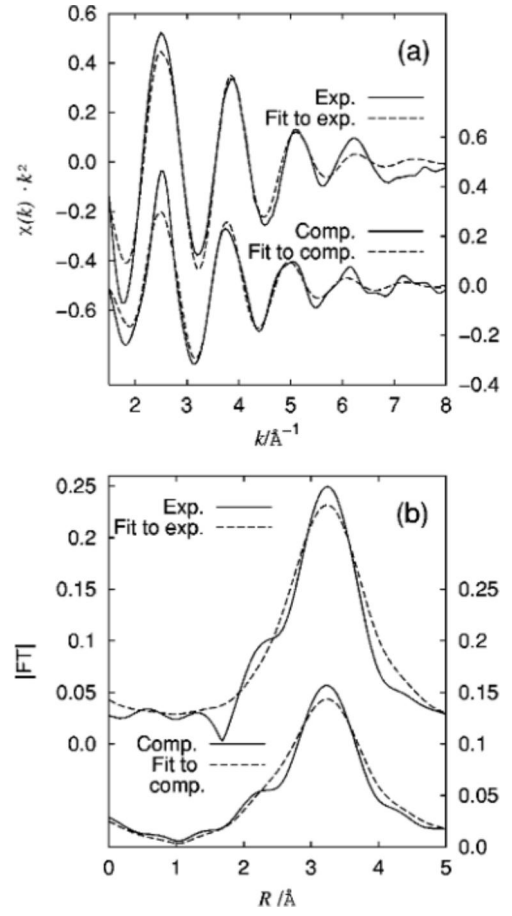

FIG. 5. (a) Experimental EXAFS spectrum and its best fit with the parameters included in Table I. (b) Phase-corrected Fourier transform of the spectrum and its fit.

in the fit procedure is shown in the "experimental" frame of Table I. As seen in the table, the values compare well with experimental results obtained by other authors. Multielectron excitations are expected around 5, 7.3, and 8.22 Å^{-1}.[38] They can be detected experimentally if the difference spectrum between experimental spectrum and fit exhibits peaks approximately at the indicated k-values. This is not the case, and therefore multielectron excitations were not included in the analysis. Some authors studying bromide concluded that multielectron excitations were not important,[38,41] while others reached a higher estimate of multielectron excitations and recommended their inclusion in the data analysis.[45,46]

The facility to handle independent structural information of statistical nature on the system under study enables us to undertake a second EXAFS data analysis which corresponds to the computed EXAFS spectrum from the MC snapshots (dashed line in Fig. 4). This type of strategy has already been performed in previous works dealing with cation hydration.[22,25] At first sight, this could be envisaged as an unnatural procedure to obtain the structural information, as the direct examination of distribution functions derived from MC seems to offer a more direct way to do it. However, the *a priori* knowledge of the structural results gives us an ideal framework to check the usual data analysis procedure to extract this information from an EXAFS spectrum. Figures 5(a) and 5(b) show the comparison between the theoretically computed spectrum and its fit. The fitted spectrum and its FT are in quite good agreement with their corresponding theoretical spectra. For the purpose of the fit, single scattering paths BrO and BrH and the multiple scattering paths BrHO and BrHOH were considered. To reduce the number of fit parameters, all DW factors for the BrO and BrH paths were assumed to be identical, as suggested by the simulation values ($\sigma^2_{\text{BrO}}=0.055$ in Table I and $\sigma^2_{\text{BrH}}=0.059$). In the case of the theoretical spectrum, the coordination number was fixed to the mean value of the simulation. S_0^2, the amplitude reduction factor, was set to 1.

The "theoretical" values given in Table I are all obtained from the Monte Carlo simulation results. The "MC simulation" line gives direct results computed from the statistical simulation. "Fit to theoretical spectrum" generates an EXAFS spectrum from the simulation snapshots and fits this spectrum, using or not the third order cumulant. These two fits run parallel to the "Fit to experimental spectrum," the main difference being that the EXAFS function analyzed is that obtained from the snapshots of the MC simulation.

In the table, the results of two fits of the theoretical spectrum can be compared: the first considers only cumulants up to second order, the second includes the third order cumulant, which is constrained with the second order cumulant value by fixing the skewness [ratio $\sigma^3/(\sigma^2)^{3/2}$] to a value of 0.37. This number arises from the simulation as explained below. The difference between the fitted BrO distances are within 0.1 Å due to the introduction of the third order cumulant. The same procedure performed on the experimental spectrum yields similar conclusions. Comparable findings were obtained by D'Angelo *et al.* in a study of bromide in methanol.[42]

The distance in the fit to the computed spectrum is 0.1 Å

TABLE I. Best fit distances, Debye–Waller factors, and coordination numbers around the bromide anion obtained from the analysis of the EXAFS spectra and of the MC simulation using 10 000 snapshots.

	N_O	R_{BrO}/Å	σ^2_{BrO}/Å^2	σ^3/Å^3
		Experiment		
Fit to experimental spectrum	5.84[a]	3.27±0.04	0.035±0.002	···
Fit to experimental spectrum with $\sigma^3=0.37(\sigma^2_{BrO})^{3/2}$	5.84[a]	3.34±0.03	0.034±0.002	0.0023±0.0002
Ref. 26	7.2±0.4	3.36±0.01	0.027±0.002	−0.0014±0.0006
Ref. 27	6.9	3.34	0.04	0.0065
Ref. 50	6[a]	3.19	0.016	···
Ref. 48	6[a]	3.20	0.022	0.0034
Ref. 41	5.1±0.5	3.29±0.04	0.026±0.03	0.0020±0.0020
		Theory		
MC simulation	5.84±0.3	3.54±0.01	0.055±0.005	0.0036±0.0002
Fit to theoretical spectrum	5.84[a]	3.37±0.03	0.037±0.002	···
Fit to theoretical spectrum with $\sigma^3=0.37(\sigma^2_{BrO})^{3/2}$	5.84[a]	3.44±0.03	0.036±0.002	0.0025±0.0004
Fit to 1st-shell PDF	7.0±0.1	3.50±0.01	0.065±0.001	···
Fit to 1st-shell PDF with σ^3	6.9±0.1	3.54±0.01	0.058±0.001	0.0052±0.0005

[a]Fixed value.

larger than the corresponding experimental one (3.44 versus 3.34). On one hand, this discrepancy could be ascribed to the molecular potential models. On the other hand, the discrepancy could arise from the fitting procedure itself as discussed below.

C. Analysis of the procedure to obtain the geometrical parameters from a nonrigid distribution around the reference atom

The EXAFS spectrum of the bromide anion in water is a conceptually interesting case for methodological studies because the spectrum is dominated by the BrO backscattering contribution. The present study corroborates that contributions from multiple scattering paths (excepted the "focusing" path BrHO) and single scattering contributions from atoms at distances larger than 5.0 Å play a minor role.[26,27] The BrO distribution of distances is, however, quite broad and asymmetric. Therefore, a model structure should be valid, if it was able to reproduce essentially the probability distribution function of the BrO distances. In this section, the analysis will be performed exclusively on the theoretically computed spectrum, so that experimental considerations do not need to be taken into account and the distribution is known. The aim is to monitor thoroughly how the EXAFS determination can reproduce the geometrical distribution, what was used reversely to generate the EXAFS spectrum.

A striking feature of the structural determination by EXAFS spectroscopy is that distances are usually slightly shorter than expected, and/or obtained by other techniques.[1] Such a difference is also observed between the distance obtained by averaging the MC simulation snapshots and the fitted distance to the theoretical spectrum (for example, $R_{BrO}=3.54$ versus 3.44 Å). In fact, the coordination distance obtained from the EXAFS fit is numerically very close to the maximum of the $g(r)$ function shown for instance in Ref. 28. This observation applies also to the case of the second shell of Rh^{3+} and Cr^{3+}.[24,25] In the bromide study, the fitted DW factors are only roughly half of the value found in the simulation (0.037 versus 0.055 Å^2), while the coordination number is maintained fixed. The systematic underestimation of distances even when the "correct" third order cumulant is used enables a slight refinement of the estimated experimental distance based on a transferability of the difference obtained from the theoretical computation. This should be warranted if the shape of the distribution of the simulation corresponds to the real one,

$$\Delta R_{theor}=R_{MC\ Simulation}-R_{Fit\ to\ theor\ with\ \sigma^3}$$
$$=3.54-3.44\ \text{Å}=0.1\ \text{Å}.$$

Then,

$$R_{exp-theor}=R_{Fit\ to\ exp\ with\ \sigma^3}+\Delta R_{theor}=3.34+0.1\ \text{Å}.$$

Therefore, our estimate of the average first shell BrO distance from the experimental spectrum is 3.44±0.07 Å.

In order to find out more about the reasons for this difference in the first hydration shell, several attempts were made using only the information about the distribution in this shell. The structural information used in all these calculations is that obtained from the MC results. Table I gives the integration number, average BrO distance and its DW factor (σ^2). For the purpose of the analysis, the BrO first peak had to be isolated somewhat arbitrarily, since the distribution function does not drop to zero. The chosen criterium was to use a switching function, centered around the minimum of the distribution function, that brings the distribution to zero arctangently between 3.8 and 4.2 Å. If a strict cutoff criterium is chosen instead, the qualitative conclusions drawn here are not affected. The reference distribution in all these calculations is given by the probability distribution function (PDF), plotted in Fig. 6 (solid line). This function is directly related to the radial distribution function ($g(R)$),

$$\text{PDF}(R_{BrO})=N(g^{sw}(R_{BrO})\cdot R^2_{BrO}), \quad (3)$$

where the superscript "sw" refers to the switched $g(R)$ and N is a normalization constant.

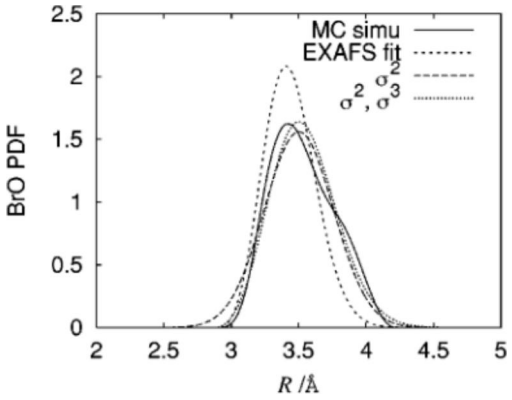

FIG. 6. BrO probability distribution functions (PDF) from MC simulation (solid line), from fit to theoretical EXAFS spectrum with σ^3 (dashed), and from two fits to the MC PDF: with cumulants up to 2 (long dashed) and up to 3 (dotted).

To follow the steps of an EXAFS data analysis, the Fourier transform of the PDF was used as input for the fit of the following expression:[47]

$$\widetilde{\mathrm{PDF}}(k) = A\ \exp(iR_{\mathrm{BrO}}k - \sigma^2 k^2/2 - i\sigma^3 k^3/6) \qquad (4)$$

which yields "effective cumulants." Table I gives two sets of results, considering or not the third order cumulant. "Fit to 1st shell PDF" uses the BrO distribution function and fits coordination number, distance, and DW factor in a manner detailed in the next section. "Fit to 1st shell PDF with σ^3" additionally fits the third order cumulant. The third order cumulant is found to be 0.0052 $Å^3$ (see Table I), that is, $0.37(\sigma^2)^{3/2}$. Constraining the skewness to a value of 0.37 in all the fits ensures that the distributions found are comparably asymmetrical. Third order cumulants finally differ greatly between authors and methods used. A direct fit to the EXAFS spectrum is subject to high uncertainties: Wallen *et al.*[26] determine a negative value, while Simonet *et al.*[41] obtain a value in agreement with those obtained by other authors using alternate approaches.[48] D'Angelo *et al.*[27] obtain a skewness of 0.81. Within their approach, however, higher order cumulants also play a significant role. In this work, a direct calculation of σ^3 from the MC simulation yields 0.0036, that is a skewness of 0.28, but if we want to neglect higher order cumulants, it is more interesting to make use of an effective value.

When second and third order cumulants are included, the average distance determined in the fit of the PDF is equal to the reference one (3.54 Å). The corresponding distribution is plotted in Fig. 6 (dotted line). When the fit includes only second order cumulants, the distance determined is 3.50 Å (long dashed line). That is, a shortening of the distance is observed. This value is quite different from the one obtained by fitting to the computed EXAFS function (3.44 or 3.37 Å, respectively).

Another test of the method for the determination of the structure lies in the investigation of the possible artifact associated to the generation of the EXAFS function via the FEFF/FEFFIT method from the snapshots of the MC simulation. Two numerical examinations have been designed. The first consisted in generating a theoretical EXAFS spectrum arising solely from single scattering contributions of the first shell of oxygen atoms. The fit included only BrO single scattering paths and second order cumulants, yielding a distance of 3.36 Å. The second examination was the generation of an EXAFS spectrum based on model structures of the geometry "c" of Fig. 1, where the position of the water molecules was symmetrically modified between 2.8 and 4.2 Å for the BrO distance. These spectra were weighted by the PDF of the first peak. This theoretical spectrum bears a close resemblance to the one obtained by the averaging of spectra from MC snapshots, and the fit parameters are very similar. This is a strong indication that the reason for the discrepancy is not due to multiple scattering effects or the presence of hydrogen atoms close to the bromide, but is rather to be found in the shape of the distribution and the inability to adjust it with DW factors.

IV. CONCLUDING REMARKS

XANES and EXAFS spectra of Br *K*-edge of bromide in water were calculated from simulation snapshots and, in the case of XANES, quantum-mechanically minimized clusters were also probed. Whereas the quantum-mechanical clusters do not compare well with experimental data in solution, the set of simulation data leads to a good agreement. The discrepancies between XANES spectra calculated from quantum-mechanical structures and MC simulations suggest the need for including statistical information in the computation. In this sense, it is essential to use a statistical distribution of water molecules around the bromide anion derived from a condensed matter system where ion–water and water–water interactions play a significant role. Bearing in mind that intermolecular potentials were fitted to *ab initio* calculations of similar level than those used for the structure optimized quantum-mechanically, the main reason to justify the difference must be the statistical factors.

In the case of the EXAFS computations of bromide hydration, the main contributions are due to single scattering from the first hydration shell and, due to this reason, can be handled realistically by a one-dimensional distribution of model structures. This is a simplified picture of the more realistic scattering phenomenon where BrHO paths and BrH paths are being considered.

The broad and asymmetric distribution of BrO distances in the simulation was described in terms of an asymmetry parameter of 0.37 (skewness) in order to be able to obtain second and third order cumulants with low indeterminations for the fit to the EXAFS spectrum. This asymmetry parameter was obtained by fitting the BrO distribution of the simulation in *k*-space.

The discrepancies that appear between the theoretical EXAFS spectrum and its fit using cumulants indicate that systems with significant geometrical disorder in the closer environment of the absorber atom, like the first hydration shell of the bromide anion, can hardly be described by cumulants limited to third (or fourth) order.[49] Due to the characteristics of the probability distribution function, distances obtained by a conventional fit procedure to the EXAFS spectrum are observed to be close to the maximum of the radial distribution function when solely DW factors are considered,

and also fall short when third order cumulants are introduced. The systematic underestimation of distances even when the "correct" third order cumulant is used enables a slight refinement of the estimated experimental distance. If we assume that the distribution of distances from the simulation is correct, we obtain that the average BrO distance determined in the experimental fit (3.34 Å) is underestimated by 0.1 Å. Therefore, our best guess of the experimental distance is 3.44 ± 0.07 Å. A combination of experimental and theoretical data analysis gives wider possibilities to investigate the geometrical properties of systems presenting ill-defined structural patterns.

ACKNOWLEDGMENTS

The authors thank Dr. A. Muñoz-Páez for her experimental collaboration and her helpful discussions. Suggestions from the referee have improved this paper. Patrick Merkling wishes to thank the Junta de Andalucía and the Deutsche Forschungsgemeinschaft for financial support. Experimental spectra were measured under proposal 95G-215 of the Photon Factory, Tsukuba, Japan. Fundación Ramón Areces (XI Concurso Nacional) is acknowledged for financial support.

[1] H. Ohtaki and T. Radnai, Chem. Rev. (Washington, D.C.) **93**, 1157 (1993).
[2] Y. Marcus, *Ion Solvation* (Wiley, Chichester, 1986).
[3] D. T. Richens, *The Chemistry of Aqua Ions* (Wiley, Chichester, 1997).
[4] M. Magini, G. Licheri, G. Paschina, G. Piccaluga, and G. Pinna, *X-Ray Diffraction of Ions in Aqueous Solutions: Hydration and Complex Formation* (CRC Press, Boca Raton, 1988).
[5] J. E. Enderby, in *Techniques for Characterization of Electrodes and Electrochemical Processes*, edited by R. Varma and J. R. Selman (Wiley, New York, 1991), Chap. 7.
[6] D. E. Sayers, E. A. Stern, and F. W. Lytle, Phys. Rev. Lett. **27**, 1204 (1971).
[7] J. Penner-Hahn, Coord. Chem. Rev. **190–192**, 1101 (1999).
[8] S. Fendorf, in *Synchrotron X-Ray Methods in Clay Science*, edited by D. Schulze, J. Stucki, and P. Bertsch (The Clay Minerals Society, Aurora, 1999), Vol. 9, p. 19.
[9] *X-Ray Absorption: Principles, Applications, Techniques of EXAFS, SEXAFS, and XANES*, edited by D. C. Koningsberger and R. Prins (Wiley, New York, 1988).
[10] J. J. Rehr and R. C. Albers, Rev. Mod. Phys. **72**, 621 (2000).
[11] Y. Joly, D. Cabaret, H. Renevier, and C. R. Natoli, Phys. Rev. Lett. **82**, 2398 (1999).
[12] B. J. Palmer, D. M. Pfund, and J. L. Fulton, J. Phys. Chem. **100**, 13393 (1996).
[13] D. Roccatano, H. J. C. Berendsen, and P. D'Angelo, J. Chem. Phys. **108**, 9487 (1998), and references therein.
[14] A. Filipponi, P. D'Angelo, N. V. Pavel, and A. Di Cicco, Chem. Phys. Lett. **225**, 150 (1994).
[15] F. Jalilehvand, D. Spångberg, P. Lindqvist-Reis, K. Hermansson, I. Persson, and M. Sandström, J. Am. Chem. Soc. **123**, 431 (2001).
[16] L. Campbell, J. J. Rehr, G. K. Schenter, M. I. McCarthy, and D. Dixon, J. Synchrotron Radiat. **6**, 310 (1999).
[17] P. D'Angelo, V. Barone, G. Chillemi, N. Sanna, W. Meyer-Klaucke, and N. V. Pavel, J. Am. Chem. Soc. **124**, 1958 (2002), and references therein.
[18] R. Ayala, E. Sánchez Marcos, S. Díaz-Moreno, V. A. Solé, and A. Muñoz-Páez, J. Phys. Chem. B **105**, 7588 (2001).
[19] S. Díaz-Moreno, J. M. Martínez, A. Muñoz-Páez, H. Sakane, and I. Watanabe, J. Phys. Chem. A **102**, 7435 (1998).
[20] J. M. Martínez, R. R. Pappalardo, E. Sánchez Marcos, K. Refson, S. Díaz-Moreno, and A. Muñoz-Páez, J. Phys. Chem. B **102**, 3272 (1998).
[21] H. Sakane, A. Muñoz-Páez, S. Díaz-Moreno, J. M. Martínez, R. R. Pappalardo, and E. Sánchez Marcos, J. Am. Chem. Soc. **120**, 10397 (1998).
[22] P. J. Merkling, A. Muñoz-Páez, J. M. Martínez, R. R. Pappalardo, and E. Sánchez Marcos, Phys. Rev. B **64**, 012201 (2001).
[23] A. Muñoz-Páez, S. Díaz-Moreno, E. Sánchez Marcos, and J. J. Rehr, Inorg. Chem. **39**, 3784 (2000).
[24] P. J. Merkling, A. Muñoz-Páez, R. R. Pappalardo, and E. Sánchez Marcos, Phys. Rev. B **64**, 092201 (2001).
[25] P. J. Merkling, A. Muñoz-Páez, and E. Sánchez Marcos, J. Am. Chem. Soc. **124**, 10911 (2002).
[26] S. L. Wallen, B. J. Palmer, D. M. Pfund, J. L. Fulton, M. Newville, Y. Ma, and E. A. Stern, J. Phys. Chem. A **101**, 9632 (1997).
[27] P. D'Angelo, A. Di Nola, M. Mangoni, and N. V. Pavel, J. Chem. Phys. **100**, 985 (1994).
[28] R. Ayala, J. M. Martínez, R. R. Pappalardo, H. Saint-Martín, I. Ortega-Blake, and E. Sánchez Marcos, J. Chem. Phys. **117**, 10512 (2002).
[29] R. Ayala, J. M. Martínez, R. R. Pappalardo, and E. Sánchez Marcos, J. Phys. Chem. A **104**, 2799 (2000).
[30] H. Saint-Martin, J. Hernandez-Cobos, M. I. Bernal-Uruchurtu, I. Ortega-Blake, and H. J. C. Berendsen, J. Chem. Phys. **113**, 10899 (2000).
[31] MCHANG program, The code is available upon request at jorge@fis.unam.mx
[32] M. Leslie and M. I. Gillan, J. Phys.: Condens. Matter **18**, 973 (1985).
[33] J. E. Roberts and J. Schnitker, J. Phys. Chem. **99**, 1322 (1995).
[34] A. Ankudinov, B. Ravel, J. J. Rehr, and S. D. Conradson, Phys. Rev. B **58**, 7565 (1998).
[35] L. Hedin and S. Lundqvist, Solid State Phys. **23**, 1 (1969).
[36] G. Ferlat, A. San Miguel, J. Jal, J. Soetens, P. A. Bopp, I. Daniel, S. Guillot, J. L. Hazemann, and R. Argoud, Phys. Rev. B **64**, 134202 (2001).
[37] J. L. Fulton, M. M. Hoffmann, J. G. Darab, B. J. Palmer, and E. A. Stern, J. Phys. Chem. A **104**, 11651 (2000).
[38] J. Chaboy, A. Muñoz-Páez, and S. Díaz-Moreno, Chem.-Eur. J. **7**, 1102 (2001).
[39] E. A. Stern, M. Newville, B. Ravel, Y. Yacoby, and D. Haskel, Physica B **208–209**, 117 (1995).
[40] H. Sakane, T. Miyanaga, I. Watanabe, N. Matsubayashi, S. Ikeda, and Y. Yokoyama, Jpn. J. Appl. Phys., Part 1 **32**, 4641 (1993).
[41] V. Simonet, Y. Calzavara, J. L. Hazemann, R. Argoud, O. Geaymond, and D. Raoux, J. Chem. Phys. **116**, 2997 (2002).
[42] P. D'Angelo, A. Di Nola, M. Mangoni, and N. V. Pavel, J. Chem. Phys. **104**, 1779 (1996).
[43] B. Lengeler, Phys. Rev. Lett. **53**, 74 (1984).
[44] R. Mayanovic, A. Anderson, W. Basset, and I.-M. Chou, Chem. Phys. Lett. **336**, 212 (2001).
[45] P. D'Angelo, A. Di Cicco, A. Filipponi, and N. V. Pavel, Phys. Rev. A **47**, 2055 (1993).
[46] P. D'Angelo and N. V. Pavel, Phys. Rev. B **64**, 233112 (2001).
[47] H. Cramer, *Mathematical Methods of Statistics* (Princeton University Press, Princeton, 1946).
[48] H. Tanida, H. Sakane, and I. Watanabe, J. Chem. Soc., Faraday Trans. **1994**, 2321.
[49] P. Lindqvist-Reis, K. Lamble, S. Pattanaik, I. Persson, and M. Sandström, J. Phys. Chem. B **104**, 402 (2000).
[50] Y. Sawa, T. Miyanaga, H. Tanida, and I. Watanabe, J. Chem. Soc., Faraday Trans. **91**, 4389 (1995).